Comprehensive two-dimensional liquid chromatography with inductively coupled plasma mass spectrometry detection for the characterization of sulfur, vanadium and nickel compounds in petroleum products

Marie Bernardin, Agnès Le Masle, Frédérique Bessueille-Barbier, Charles-Philippe Lienemann, Sabine Heinisch

Comprehensive two-dimensional liquid chromatography with inductively coupled plasma mass spectrometry detection for the characterization of sulfur, vanadium and nickel compounds in petroleum products

Marie Bernardin[1,2], *Agnès Le Masle*[2], *Frédérique Bessueille-Barbier*[1], *Charles-Philippe Lienemann*[2], *Sabine Heinisch**[1]

(1) Université de Lyon, Institut des Sciences Analytiques, UMR 5280, CNRS, 5 rue de la Doua, 69100 Villeurbanne, France

(2) IFP Energies nouvelles, Rond-point de l'échangeur de Solaize, BP 3, 69360 Solaize France

* Corresponding author: Tel: +33 437 423 551;

E-mail address: sabine.heinisch@univ-lyon1.fr (Sabine Heinisch)

Abstract

The petroleum industry is increasingly concerned with the conversion of vacuum residues as a consequence of decreased conventional crude oil availability. The compositional analysis of heavy oil products has become a key step in conversion processes, but the complexity of these oil matrices tends to increase with their boiling point. In this study, comprehensive two-dimensional liquid chromatography (LCxLC) coupled to inductively coupled mass spectrometry (ICP-MS/MS) is considered with a view to meet new requirements and to bring additional information regarding the species present in these matrices. In search for a high degree of orthogonality, two separation techniques involving two different retention mechanisms were evaluated: Size Exclusion Chromatography (SEC) and Reverse Phase Liquid Chromatography (RPLC). In SEC, the analytes are separated according to their molecular weight while according to their hydrophobicity in RPLC. The separation power of both individual separation techniques was first evaluated. Off-line and on-line LCxLC were compared on the basis of an optimization approach. It is shown that off-line SECxRPLC can provide, for the same analysis time of 150 min, a higher peak capacity (2600 vs 1700) while a similar dilution factor (close to 30) but also requires far fewer fractions to be analyzed (12 vs

400). Asphaltenes which constitute the heaviest fraction of crude oils (obtained from petroleum industry) were analyzed by the developed off-line SECxRPLC method. The resulting 2D-contour plots show that co-elutions could be removed leading, for the first time, to new information on high molecular weight species containing sulfur and vanadium.

Keywords:

SECxRPLC; Peak capacity; Heavy oils; Organic matrices; Speciation; ICP-MS/MS

1. Introduction

As the production of conventional middle and light oils has been declining over the last decades, heavy crude oils are increasingly used in the petroleum industry to replace them [1]. Crude oil is a complex mixture containing heteroatoms such as sulfur, and heavy metals like nickel and vanadium [2]. Vanadium and nickel are known to be present in petroleum up to few hundred parts per million [3,4]. To improve demetallation and hydrodesulfurization processes, a better understanding of metal speciation is necessary, which has led to a growing interest in hyphenated techniques, which can combine the high separation power of ultra-high performance liquid chromatography (UHPLC) to a specific detection such as inductively coupled plasma mass spectrometer (ICP-MS/MS). Up to now, the structural identification of the chemical species present in the matrix is far from being comprehensive. Porphyrins, chelated with nickel and vanadyl, are widely described in the literature [5–9]. However, other compounds which represent up to 80 % of the metal complex, are much more abundant than metalloporphyrins while poorly described yet [3,6], and could be found as porphyrins trapped in nanoaggregates [10,11]. Recently, several reviews have dealt with metal speciation in crude oil and heavy petroleum fraction [2,3,12]. One of the main reported analytical approaches is size exclusion chromatography coupled to ICP-HRMS (SEC-ICP-HRMS) [10,13–17]. The compounds being separated according to their hydrodynamic volumes, the catalyst pore size can be adapted according to the size of metal complexes, which can be useful for hydrodemetallation and hydrodesulfurization processes [3]. The resulting elution profiles usually consist in up to three large unresolved peaks [18,19]. Reverse Phase Liquid Chromatography (RPLC) separation was also reported for the analysis

of metalloporphyrins [20], and asphaltene fractions [21]. From all reported studies, it is clear that one-dimensional chromatography fails to provide enough separation power for a complete characterization of such very complex matrices. A few approaches were developed using two-dimensional liquid chromatography (2D-LC) for the analysis of vanadium and nickel. They combined size exclusion chromatography and Normal Phase Liquid Chromatography (NPLC) to get relevant information on both molecular weight and chemical specie polarity. Three [22] or four fractions [23] were collected from the SEC dimension and further sent to the second NPLC dimension. Although this analytical approach did not allow the complete speciation of crude oils, it could point out three metal-groups of different polarities.

In the present study, we explored the feasibility and the potential of comprehensive two-dimensional liquid chromatography (SEC combined with RPLC) coupled to ICP-MS/MS for a better characterization of such complex matrices. With organic matrices, the presence of organic solvents requires the addition of oxygen into the plasma to avoid carbon deposit onto the cone surface and plasma instabilities. In addition to this, a more critical issue with RP gradients in the second dimension stems from the continuous change in solvent composition, resulting in signal fluctuations during the run. Although different approaches were proposed, such issue is still partly solved [24–30]. For instance, some authors suggested the use of a post column counter gradient prior to ICP-MS detection [29], or isotope dilution [30]. A 2D-configuration with RPLC (gradient conditions) in the first dimension and SEC (isocratic conditions) in the second one is expected to be more attractive with respect to both separation power and peak intensities considering that, under isocratic conditions, (i) plasma instabilities are less significant and (ii) optimized plasma parameters are easier to find. A theoretical study was therefore carried out to select the best comprehensive 2D-configuration (SECxRPLC or RPLCxSEC). We made use of a calculation approach previously developed for optimizing physical parameters in LCxLC with a view to maximizing the peak capacity while minimizing the dilution within a given analysis time [31,32]. This approach also allowed us to choose between on-line and off-line mode. Whereas the off-line mode is more time-consuming, less suitable for automation, and more prone to sample loss and carry over, it should offer some advantages for our purpose: (i) a simple conventional HPLC systems can be used, (ii) after collection, the injection of the

fractions into the second dimension can be delayed making a fraction treatment possible, (iii) the same instrument can be used in both dimensions and above all (iv) the analysis time in the second dimension is not limited [34].

The first part of this work was devoted to the selection of appropriate conditions for the first and the second dimensions, both in off-line and on-line mode. As a result of this optimization procedure, off-line SECxRPLC-ICP-MS/MS was applied to the analysis of the sub-fractions of heavy crude oils. The obtained results could provide new information on high molecular weight species containing sulfur and vanadium.

2. Experimental section

2.1. Chemicals and reagent

Tetrahydrofuran (LC-MS grade), acetonitrile (LC-MS grade), 2,3,7,8,12,13,17,18-Octaethyl-21H,23H-porphine vanadium(IV) oxide standard were purchased from Sigma Aldrich (Steinheim, Germany). Ethyl acetate was purchased from Carlo Erba (Val-de-Reuil, France). 1-Methyl-2-pyrrolidinone were purchased from Fisher Scientific (Illkirch, France). Water was obtained from Elga water purification system (Veolia water STI, Le Pless Robinson, France). SPEX CertiPrep (Metuchen, NJ, USA) Co, Ce, Y, Tl, Li monoelemental standards in 2 % HNO_3 (1000 µg/L) were used daily for the ICP-MS/MS system calibration. A multi-element solution containing Co, Ce, Y, Tl, Li at 10 ppb in acetonitrile was used to monitor the instrument. 8 polystyrene standards were used in 2 different solutions. Solution A contains PS of 28000, 9130, 682 and 266 Da, solution B contains PS of 44000, 15700, 3470, and 1250 Da in THF. Polystyrene standards were supplied by Fluka Analytical, Sigma Aldrich (Steinheim, Germany).

2.2. Sample preparation

Analyzed samples came from Vacuum Residues (VRs) obtained after atmospheric distillation and vacuum distillation in the refining process of crude oil. To simplify the matrix, VRs have been fractionated according to a two-step SARA method [3], as shown in Fig.1. Asphaltenes were first precipitated with a non-polar solvent (n-heptane). The fractionation of the maltenes was then performed by column chromatography resulting in SARA fractions (Saturates, Aromatics, Resins, and Asphaltenes). Those were supplied by IFPEN. SARA

fractions were then diluted 60-times v/v in THF before being analyzed. An atmospheric residue (AR Venezuela), supplied by IFPEN and diluted 60 times, was also used for the evaluation of the performance of SEC-ICP-MS.

2.3. Instrumentation

2.3.1. LC system

The instrument was an Infinity 1290 LC from Agilent Technologies (Waldbronn, Germany). It includes a high-pressure binary solvent manager with a maximum flow-rate of 5 mL/min, an auto-sampler with a flow-through needle device equipped with a 20 µL sample loop, a column oven with a maximum temperature of 100 °C. The measured dwell volume was 300 µL. The instrument control was performed by Mass Hunter. A UV detector equipped with 2 µL flow-cell was used for experiment described section 3.1. Detector wavelength was set at 407 nm. The same LC instrument was used in the two dimensions. The outlet of the column was connected to a T-union P-727 (from Upchurch, Cluzeau, Sainte-Foy-La-Grande, France) with zero dead volume. Only stainless steel tubing was used for THF compatibility. Tube #1 (50 cm x 125 cm) was located between the column and the T-union, Tube #2 (20 cm x 125 µm) between the T-union and the Sample Introduction System (SIS) prior to the ICP-MS/MS, Tube #3 (25 cm x 125 µm) between the T-union and the waste. The split ratio was set to 1:1 to ensure proper conditions (400 µL/min) for the nebulizer. SEC column calibration was performed with a diode array detector equipped with 0.6 µL flow-cell, from Agilent Technologies (Waldbronn, Germany).

2.3.2. ICP-MS/MS

The experiments were carried out using an Agilent 8800 ICP-MS/MS system from Agilent Technologies (Waldbronn, Germany) with a PFA-LC nebulizer from Elemental Scientific (Omaha, Nebraska USA), an IsoMist device from Courtage Analysis Service (Mont Saint Aignan, France), equipped with a Twinnabar spray chamber as Sample Introduction System (SIS), selected according to previous studies [35,36]. The spray chamber was thermostated at -2 °C by Peltier effect. The system was equipped with a quartz torch with a 1 mm i.d. injector (Agilent Technologies). The following ICP-MS/MS parameters were selected: plasma power of 1500 W, auxiliary gas flow-rate of 0.9 L/min, plasma gas flow-rate of 15 L/min, sampling depth of 7 mm, carrier gas of 0.45 L/min. Viton® tubing (SCP Science, Villebon-sur-Yvette,

France) were used for correct use of the peristaltic pump under organic solvent conditions. In order to ensure plasma stability and to avoid carbon deposit on the cone surface (sampler and skimmer), 0.5 L/min of a mixture of Oxygen and Argon (20 % O_2, 80% Ar) was sent through HMI tubing into ICP-MS/MS. Both sampling and skimmer cones were made of platinum, due to its inertness, instead of usual nickel. The amount of oxygen, depending on the mobile phase (type of organic solvent and flow-rate) was optimized by visually monitoring C_2 emission band. The analyzer unit of the instrument consisted of two quadrupole mass analyzers and an octopole collision-reaction cell located between them. Vanadium, sulfur, and nickel were detected in MS/MS mode with O_2 as reaction gas in the cell. Vanadium 51 was shifted to mass 67 ($^{67}VO^+$), Sulfur 32 to mass 48 ($^{48}SO^+$). Nickel was analyzed at m/z = 58 ($^{58}Ni^+$).

To maximize the instrument sensitivity, the flow-rate of O_2 reaction gas was optimized by monitoring $^{67}VO^+$ intensity of a porphyrin sample (1 ppm in ACN) while changing the mobile phase flow-rate within 0.1 to 0.8 mL/min (see supplementary information S1). The highest sensitivity was achieved at 0.3 mL/min O_2.

The same approach was applied to the nickel and sulfur elements. O_2 reaction gas flow-rate was optimized by monitoring both $^{48}SO^+$ and $^{58}Ni^+$ intensities (100 ppb of mono-elemental standards of nickel and sulfur diluted in THF) (see supplementary information S1). The highest sensitivity was achieved at 0.2 and 0.25 mL/min O_2 respectively. The MS/MS mode was essential for sulfur analysis to avoid isobaric interference such as O_2^+. As a result, the analysis of the three elements (sulfur, vanadium, and nickel) could be performed within one single run at 0.3 mL/min O_2.

2.3.3. SEC-ICP-MS/MS setup

Two Waters APC columns were used: an ACQUITY APC XT 45 (150 x 4.6 mm, 1.7 µm) with effective molecular weight ranging from 200 to 5000 g/mol and an ACQUITY APC XT 125 (150 x 4.6 mm, 2.5 µm) with effective molecular weight ranging from 1000 to 30000 g/mol. For both columns, the injection volume was 15 µL. The column temperature was set to 30 °C. THF was used as mobile phase. The mobile phase flow-rate was 0.8 mL/min. A flow-splitter (1:1) was used prior to the ICP-MS/MS detector.

2.3.4. RPLC-ICP-MS/MS

Several stationary phases were evaluated in RPLC. Those are listed in Table S1. The column temperature was set at 30 °C. Acquity BEH C_{18}, Vydac C_{18}, Hypersil Betabasic were operated at a flow-rate of 0.8 mL/min. Zorbax-SB-CN was operated at a flow-rate of 1 mL/min. 80/20 ACN/H_2O (v/v) was used as mobile phase (A) and THF was used as mobile phase (B). A linear gradient was applied from 1% B to 99% B, keeping a normalized gradient slope of 5 % (gradient slope x column dead time). The injection volumes are given in Table S1. Flow-splitting (1:1) was used prior to the ICP-MS/MS detector.

2.3.5. SECxRPLC-ICP-MS/MS setup

In off-line SECxRPLC, an ACQUITY APC XT 125 (150 x 4.6 mm, 2.5 µm) column and an ACQUITY BEH C_{18} (50 x 2.1 mm, 1.7 µm) column were used in the first (^{1}D) and second (^{2}D) dimensions respectively. The injection volumes were 15 µL and 5 µL respectively. The column temperature was set at 30 °C in both dimensions. ^{1}D mobile phase was THF. ^{2}D mobile phase was ACN/H_2O, 80/20, (v/v) (A), and THF (B) with the following gradient program: 0-10.2 min, 1 % B to 99 % B; 10.2-15.2 min, 99 % B; 15.2-15.3 min, 99 % to 1 % B; 15.3-15.8 min, 1 % B, leading to a normalized gradient slope of 1.2 %. In both dimensions the flow-rate was 800 µL/min with a flow-splitter of 1:1 prior to the ICP-MS/MS detection. Fractionation was manually performed every 10 s since no fraction collector was compatible with THF at the time of the present study. The filled vials were directly placed into the auto-sampler to be further analyzed in the second dimension. No fraction treatment was performed between both dimensions.

2.4. Calculations

The peak capacity, n, was first introduced by Giddings to provide a valuable tool capable of assessing the separation power. It was defined as the number of peaks that can be ideally placed between the first peak and the last peak of interest with a resolution of 1.0 between all peaks [37]. In RPLC and in gradient elution, the peak capacity, n_{RPLC}, can be calculated according to [38]:

$$n_{RPLC} = 1 + \frac{\sqrt{N_{measured}}}{4} \cdot \frac{1}{2.3b+1} \cdot ln\left(\frac{2.3b+1}{2.3b} \cdot e^{2.3S\Delta Ce} - \frac{1}{2.3b}\right) \quad (1)$$

Where S is the average slope of the relationship between the logarithm of the retention factor and the solvent composition. It can be estimated from the molecular mass, according

to an empirical relationship, ΔCe is the range of compositions at elution covered by the sample, $N_{measured}$, the measured plate number which may differ from the column plate number due to extra-column dispersion [32] and b is the Linear Solvent Strength (LSS) gradient steepness [39], defined as:

$$b = \frac{S.\Delta C.t_0}{t_G} \quad (2)$$

With ΔC the gradient composition range, t_G the gradient time and t_0 the column dead time.

In size-exclusion chromatography (SEC), solutes are ideally eluted according to their decreasing size. When considering that the peak width is approximately constant, and that the components are spread over the entire elution space, the peak capacity may be expressed as Eq.(3) [40]:

$$n_{SEC} = 1 + \left(\frac{V_0 - V_e}{V_0}\right)\frac{\sqrt{N_{measured}}}{4} \quad (3)$$

Where V_0 is the total permeation volume (column dead volume) and, V_e, is the total exclusion volume. The peak capacity can also be related to the total porosity, ε_t, and the external porosity, ε_e:

$$n_{SEC} = 1 + \left(\frac{\varepsilon_t - \varepsilon_e}{\varepsilon_t}\right)\frac{\sqrt{N_{measured}}}{4} \quad (4)$$

The sample peak capacity in LCxLC is theoretically the product of sample peak capacities in each dimension:

$$n_{2D} = {}^1n \times {}^2n \quad (5)$$

Where ${}^1n$ and ${}^2n$ are the peak capacities in first and second dimension respectively. The superscript "1" and "2" refers to the first and second dimension respectively.

In LCxLC, the expected effective peak capacity is affected by three correction factors:

$$n_{2D,effecttive} = \alpha(1-\gamma)\,{}^1n + \alpha \cdot \beta \cdot \gamma \cdot {}^1n \cdot {}^2n \quad (6)$$

With α correcting the peak capacity in ^{1}D due to undersampling, β correcting the peak capacity in ^{2}D due to non-ideal transfer of the sample fraction from ^{1}D to ^{2}D [41], and γ taking into account the retention surface coverage which depends on the degree of orthogonality between both dimensions [42]. In off-line mode, α and β can attain values very close to 1. This is made possible by increasing the number of fractions per peak in order to

reduce both under sampling (increasing α) and injection issues (increasing β). The fractions can be stored and analyzed in ^{2}D at a later time after a possible treatment (i.e. solvent evaporation and dilution in a weaker solvent).

The conditions for LCxLC analysis were optimized using a home-made procedure developed with Microsoft Excel. The calculations were based on a Pareto-optimal approach with the aim to optimize, for a given analysis time, two conflicting criteria, minimizing the dilution factor while maximizing the peak capacity [31].

The dilution factor, D_f, in dimension "i" was calculated according to the following equation:

$$D_f = \frac{\sqrt{2\pi}}{\beta} \times \frac{{}^{i}\sigma_{v\,col}}{{}^{i}V_{inj}} \quad (7)$$

Where ${}^{i}V_{inj}$ is the injection volume, ${}^{i}\sigma_{v\,col}$ is the peak standard deviation in volume units and can be expressed as:

$$\sigma_{v,col} = \frac{V_0\,(2.3b+1)}{2.3b\sqrt{N_{col}}} \quad (8)$$

N_{col} was evaluated from the coefficient of the Knox equation:

$$N_{col} = \frac{L_c}{d_p} \times \frac{1}{h(u)} \quad (9)$$

$$\text{With } h(u) = au^{0.33} + b\frac{D_m}{ud_p} + c\frac{ud_p}{D_m} \quad (10)$$

With L_c the column length, u the linear velocity, d_p the particle size, D_m the diffusion coefficient, and a, b and c, the Knox's coefficients. The average diffusion coefficient value was evaluated at 1.6 10^{-10} m²/s in water at 25°C, considering an average molecular mass of 4000 Da [43].

3. Results and discussion

3.1. Development of one-dimensional separations

For this study, Acquity APC columns were preferred to Gel Permeation Chromatography (GPC) columns that are most often used. These columns are based on polymer material, while APC columns are based on silica and possess smaller dimensions. As a result, for the

same flow-rate, the analysis with Acquity APC columns is faster while the solvent consumption is reduced.

The compounds present in heavy oil matrices are within a very wide range of molecular weights. We therefore tested two different pore sizes (45 Å and 125 Å, corresponding to the APC XT 45 and APC XT 125 columns, respectively). The elution profiles obtained with these two different columns and for the three elements of interest (sulfur, vanadium, and nickel) are represented in Fig.3. With the APC XT 45 column (Fig.3a), designed for effective molecular weights ranging from 500 to 5000 g/mol, all compounds were eluted between 1.2 min (exclusion volume of 960 µL) and 1.86 min (permeation volume of 1490 µL). With the APC XT 125 column (Fig.3b), designed for effective molecular weights ranging from 1000 to 30000 g/mol, the compounds were better distributed over the entire separation window, between 1.2 min (960 µL) and 2.3 min (1840 µL). Very small molecules, as the suspected metalloporphyrins, were better separated on the APC XT 45 column. However, the APC XT 125 column was selected for the rest of our study for two main reasons: (i) the elution space on the APC XT 125 column was much larger (880 µL vs 530 µL) and (ii) large compounds, which were less studied than metalloporphyrins in previous reported studies, were better separated. This column was calibrated with 8 polystyrenes (PS) standards (molecular weights ranging from 266 to 44000 Da) (Fig.4). PS were detected by UV detection at 254 nm. The exclusion volume corresponding to the elution of the largest PS (44000 Da) was found to be 960 µL (ε_e = 0.38) while the total permeation volume corresponding to the elution of the smallest PS (262 Da) was found to be 1840 µL (ε_t = 0.74). The corresponding fitting curve is represented in green in Fig.4 ($Y = -3.7928x^3 + 14.958x^2 - 21.058x + 14.248$). Accordingly, it is interesting to observe by comparing Figs. 3 and 4 that the average mass can be estimated at about 4000 Da and that the petroleum sample occupies the entire elution space (from 960 to 1840 µL). As a result, considering Eq.3 (with h=3), the maximum peak capacity value can be estimated at 18.

RPLC was selected as an alternative dimension because the retention mechanism is quite different from that in SEC and both may therefore lead to a high degree of orthogonality. In RPLC, the molecules are separated according to their hydrophobicity which was promising to achieve a high degree of orthogonality between both dimensions. Different stationary phases were tested by injecting the asphaltene fraction diluted in THF. The stationary phases

differed by the length of the grafted chain (i.e. C_{18} or C_8), by the type of the grafted chain (i.e. cyanopropyl or alkyl), by the pore size (i.e. 80 to 300 Å) and by the type of C_{18} (i.e. hybrid silica as the Acquity BEH C18 column or polymeric grafting as the Vydac column). The different column characteristics are reported in Table S1. For Vydac C18, Zorbax-SB-CN and Hypersil Betabasic columns, a generic gradient, from 1 % to 99 % B was applied with a normalized gradient slope of 5 % (gradient slope x column dead time). For the Acquity BEH C18 column, the same gradient was used but with a normalized gradient slope of 1%. Solvent A was 80/20 ACN/H_2O (v/v) and Solvent B, pure THF. The separations with specific detections for the three elements as well as with UV detection are shown in Figs.S2a, S2b, S2c and S2d for the four columns respectively. The separations are almost similar whatever the column. However, both Zorbax SB-CN and Acquity BEH C18 exhibit a bimodal separation for sulfur and vanadium. In addition, a bimodal separation also appears for nickel with Acquity BEH C18. For this reason and due to the small available column dimensions (particle size and column length, suitable for a second dimension) Acquity BEH C18 was selected for the rest of this study. Different organic solvents, including N-Methyl-2-pyrrolidone (NMP), ethyl acetate, tetrahydrofuran (THF) and acetonitrile (ACN) were tested as solvent B (100 %B). Strong solvents can lead to a total dissolution of petroleum samples and are more prone to a high recovery rate from the column. The objective was therefore to achieve a maximum recovery rate with 100 %B. Ethyl acetate was not suitable for the coupling of UHPLC with ICP-MS/MS due to its chemical incompatibility with the tubing used for the peristaltic pump. NMP was suitable in term of recovery but its high viscosity, without increasing the system temperature at more than 80 °C [44], prevents from working at high flow-rates. ACN was too weak to elute the entire sample from the column. THF was finally found to be the most relevant for dissolving the petroleum matrix as well as for being used as solvent B. A mixture of ACN and water (80/20 ACN/H_2O) was selected as Solvent A in good agreement with a preceding study [21].

The performance of both SEC-ICP-MS/MS and RPLC-ICP-MS/MS analysis was evaluated by measuring the recovery of sulfur, vanadium, and nickel with and without column (five consecutive injections). The recovery rates for sulfur, vanadium and nickel were 104 %, 77 %, 70 % respectively in SEC while 99 %, 70 %, 67 % in RPLC. The relative standard deviations were close to 5 % in all cases. In SEC, the low recovery rate obtained for vanadium and nickel

suggests that a significant part of the related compounds was retained on the APC XT 125 column, much likely due to adsorption mechanism on the silica surface. Similar observations for vanadium and nickel were reported by *Caumette et al.* using GPC columns on petroleum sample [22]. In contrast, sulfur compounds exhibit a very good recovery rate (close to 100 %), indicating that any occurring interaction is not strong enough to result in irreversible adsorption. The recovery rates were similar in RPLC-ICP-MS/MS, supporting the idea of partial adsorption of vanadium and nickel compounds on the active silica sites while no strong adsorption exists with sulfur compounds.

Fig.5 shows the separations of SARA fractions in SEC-ICP-MS/MS for sulfur (Fig.5 a), vanadium (Fig.5b), and nickel (Fig.5c) and in RPLC-ICP-MS/MS for sulfur (Fig.5d), vanadium (Fig.5e), and nickel (Fig.5f). In both SEC and RPLC, the three elements were detected in the resin fraction (black chromatogram) and in the asphaltene fraction (green chromatogram). In the aromatic fraction (red chromatogram), only sulfur was detected. In the saturate fraction (blue chromatogram) a very small peak was found in SEC which was not detected in RPLC. It is important to note that the detection of nickel was difficult, especially in RPLC where the mobile phase was composed of THF but also of ACN and water.

In SEC, the elution profile is quite different between resin and asphaltene fractions. Asphaltenes are mostly constituted of heavy compounds or aggregates, which leads to an intense peak between 1.1 and 1.8 min. In contrast, the presence of lighter components in resins explains the intense peak at 2.3 min, close to the permeation volume, especially for vanadium (Fig.5b). A similar retention time was found for a porphyrin standard, analyzed in the same conditions, as can be observed by the overlaid dotted chromatogram in Figs.5a, 5b, and 5c. The peak at 2.3 min was therefore suspected to correspond to porphyrin compounds. By comparing Fig.5b and Fig.5c, it seems that vanadium porphyrins could be more abundant than nickel porphyrins, especially in resin fractions. This assumption will have to be confirmed in the future with quantitative analysis. Finally, as told before, column adsorption is clearly highlighted in case of asphaltenes both for vanadium and nickel which is supported by the absence of baseline return after the total permeation volume (2.3 min). Unlike other elements, sulfur is also present in aromatics with a different elution profile from those of resins and even more asphaltenes (Fig.5a), suggesting that heavy sulfur components are no more present in aromatics fraction. Asphaltenes seem to be more

enriched in vanadium and nickel than resins, which is in good agreement with reported studies [13].

As in SEC, the RPLC elution profile consists in a continuum without any isolated peak, whatever the SARA fraction. Nevertheless, a large majority of compounds is eluted with a large amount of THF, indicating that sulfur, vanadium and nickel structures are constituted of highly hydrophobic compounds, except in the aromatic fraction (red chromatogram, Fig.5d), where all compounds are eluted before 9 min. This is not surprising considering their smaller structures compared to those of the resin or asphaltene fractions. A vanadium porphyrin standard was injected separately in the same RPLC conditions (dotted chromatograms in Fig.5). Its retention time was found to be 2.6 min suggesting that porphyrin compounds were slightly retained in RPLC in these conditions. A poorly intense peak can be observed for vanadium (Fig.5e) in this retention range which could be therefore attributed to porphyrin structures. The poor intensity is mainly due to low ICP-MS/MS sensitivity in this medium (optimization performed in pure THF). It should be noticed that the elution profiles of the three considered elements are shifted towards lower retention times from asphaltenes (green chromatogram) that are more hydrophobic to aromatics (red chromatogram) that are more polar.

The use of SEC or RPLC alone cannot lead to the separation of one component from all the others due to the complexity of the matrix, constituted of hundreds of thousands compounds. As was observed in both techniques, the elution profile corresponds to a continuum regardless of the element. Yet, from the above results, the combination of RPLC and SEC was promising. The potential of SECxRPLC-ICP-MS/MS for the characterization of VRs samples and their fractions is discussed in the two following sections.

3.2. Development of two-dimensional separations

In this section, the potential of combining RPLC and SEC with a view to selecting the best configuration (SECxRPLC or RPLCxSEC) is theoretically evaluated using a predictive approach that takes into account the above results. Three important performance criteria were considered including (i) the effective peak capacity, (ii) the dilution factor and (iii) the analysis time. Both the off-line and the on-line modes were considered for that purpose. In

our quest for optimized 2D-conditions, we had to keep in mind both the instrument constraints and the available columns geometries. Those are listed below:

(1) In SEC, the available APC XT 125 column lengths were 3 cm, 7.5 cm, and 15 cm, always with an internal diameter of 4.6 mm. The maximum recommended flow-rate was 1600 µL/min. Due to partial adsorption, as previously discussed, the total analysis time had to be at least 40 % higher than the total permeation time for baseline return.
(2) In RPLC, BEH C_{18} columns are available in various lengths, various internal diameters, and various particle sizes. In this optimization study, we considered 3 different lengths (3 cm, 5 cm and 15 cm), 2 different internal diameters (2.1 mm and 4.6 mm) and 2 different particle sizes (1.7 µm and 5 µm).
(3) In order to avoid peak distortion, the maximum injected volume was found to be 1.5 % V_0 in SEC and 5 % V_0 in RPLC (V_0 being the column dead volume).
(4) Off-line fractionation was handmade due to non-compatibility of collector with THF. For the sake of convenience, the sampling time was therefore fixed to 10 s or higher.
(5) The split ratio between the first and the second dimension was not considered below 1/10 to avoid too much additional band broadening due to low split ratios as previously highlighted [35].

Under such constraints, on-line SECxRPLC was of little interest due to only one available internal diameter for SEC columns (i.e. 4.6 mm) which made very low split ratios necessary prior to the second RPLC dimension operated with usual UHPLC columns (i.d. 2.1 mm). Indeed, it was shown that such low split ratios (<1/5-1/10) can lead to a significant additional peak broadening [35], thereby substantially decreasing the effective peak capacity. Similarly, off-line RPLCxSEC was also not possible because in that case, a very large number of fractions should be collected which was beyond the capacity of the vial rack. Furthermore, the mobile phase was little compatible with the RPLC mobile phase composed partly of THF. Consequently, our choice was made between on-line RPLCxSEC and off-line SECxRPLC.

In off-line LCxLC the two dimensions are disconnected. As a result, the peak capacity in each dimension is only limited by the maximum column length that can be used considering the maximum pressure delivered by the instrument and withstood by the column. Thus, in case of two fully orthogonal LC-systems, the peak capacity in off-line LCxLC can theoretically be quite impressive. However considering the resulting huge number of runs and hence the

very long analysis time and the high associated dilution, a good trade-off has to be found between a high separation power, a reasonable analysis time and a good sensitivity. We therefore focused on the same total analysis time of about 150 min, no matter it was off-line SECxRPLC or on-line RPLCxSEC.

Our first choice was on-line RPLCxSEC. This configuration seemed to be very attractive because the second dimension is not performed in gradient elution but in pure THF. Optimized values for ICP-MS/MS parameters are fully dependent on the mobile phase composition. As a result, once they have been optimized for a given composition (e.g. 100 %THF), they may be inappropriate for compounds eluting during the gradient run in a mixture composed of water and acetonitrile in addition to THF. Furthermore, we found that the the signal intensity was higher with pure THF than with any mixture of ACN/water/THF. The same pareto-optimality approach as the one previously developed [31,32] was applied to search for optimized conditions in on-line RPLCxSEC, considering a gradient time of 150 min in the first dimension. This was achieved by varying ^{1}D column length (15; 5 and 3 cm), ^{1}D particle size (5 and 1.7 µm) ^{1}D column internal diameter (4.6 and 2.1 mm), ^{1}D flow-rate (from 10 to 500 µL/min), ^{1}D split ratio (from 1 down to 1/10), ^{2}D column length (15; 7.5 and 3 cm), ^{2}D column temperature (30 and 60 °C), ^{2}D flow-rate (from 800 to 1600 µL/min) and the sampling rate (from 1 to 3 fractions per peak). The resulting pareto plots, considering a full occupation of the retention space (γ=1) are shown in Fig.6. On-line mode usually involves the use of short second dimension columns. In our case, only a very short SEC column (i.e. 3 cm) operated at the maximum allowed flow-rate (i.e. 1600 µL/min) and at the maximum allowed temperature (i.e. 60 °C) provided enough time to carry out the separation. Among all the different sets of conditions represented by red triangles in Fig.6, some of them, located on the pareto-optimal front (red dotted line), are of prime interest. Conditions and performance of optimized settings numbered #1 to #5, are detailed in Table 1. Setting #1 is expected to provide the highest effective peak capacity (1700), despite a high dilution factor (i.e. 25) whereas setting #5 should lead to the lowest peak capacity (1000) but with a more satisfactory dilution factor (i.e. 3). It is interesting to note that for the 5 sets of optimized conditions, only a column internal diameter of 2.1 mm seems to be appropriate in ^{1}D. Increasing ^{1}D column length has a negative impact on effective peak capacity while a positive one on dilution. As shown by the results listed in Table 1, the number of runs in the second

dimension is quite impressive (300 to 450). Moreover, the split ratio is 1/5 or lower, which could result in a decrease in the effective peak capacity due to additional peak broadening. It should also be noted that an additional issue with SEC in the second dimension was raised by Reingruber et al. [45]. The injection solvent in SEC (i.e. the first dimension mobile phase), is composed of a mixture of ACN, water, and THF, and hence is prone to produce adsorption phenomena in SEC and hence significant peak tailing.

Our second choice was off-line SECxRPLC. The conditions were imposed by the constraints we had to deal with. The best set of conditions, considering the necessity of fractionating every 10 s, is represented by a blue circle in Fig.6. The related conditions are listed in Table 2. 12 fractions were collected between 1 and 2 min. The gradient time in the second dimension was set at 10.2 min so that the total analysis time was close to 150 min. Under such conditions, the calculated effective peak capacity is 2600, much higher than in on-line RPLC x SEC (<1700) whereas the dilution factor is quite similar to the one calculated for setting #1 (27 vs 25).

Considering the huge number of runs in on-line RPLCxSEC without any significant gain in effective peak capacity or in sensitivity compared to off-line SECxRPLC, on line RPLCxSEC was abandoned and off-line SECxRPLC was definitely selected to analyze complex samples coming from the petroleum industry.

3.3. Analysis of the SARA fractions by SECxRPLC-ICP-MS/MS

SARA fractions were analyzed by off-line SECxRPLC-ICP-MS/MS with conditions listed in Table 2. Fig.7 shows the 2D-contour plots for the fractions of aromatics, resins and asphaltenes considering the sulfur and vanadium elements. As told before, this 2D-set-up associates hydrophobicity property to mass property. Large compounds, early eluted in SEC are strongly retained in RPLC, likely due to the presence of a large number of carbons. Unfortunately, too much dilution in LCxLC (as above discussed) prevented from detecting nickel, present at a very low level. For the same reason, vanadium could not be detected in the aromatic fraction. 2D-contour plots are significantly different depending on both the fraction and the element. For the asphaltene fraction, in case of both sulfur (Fig.7c) and vanadium (Fig.7f), whereas there is no baseline separation in SEC, a bimodal distribution with baseline separation appears in RPLC for the most retained compounds. This suggests

that both sulfur and vanadium compounds are present in two different families differing by their hydrophobicity. Structural identification by NMR as well as LCxLC-MS analysis should be carried out to get additional information on these compounds, which should be of great interest for the petroleum industry.

In order to underline the main differences between the SARA fractions, the contours of the 2D-contour plots are overlaid for sulfur (Fig.8a) and for vanadium (Fig.8b). As can be seen, each SARA fraction has its own contour, with a form different depending on the fraction. In case of sulfur as example (Fig.8a), the form related to aromatics suggests the presence of lighter compounds compared to resins and asphaltenes. It can also be noted that the contour of resins is included into the one of asphaltenes both in case of sulfur and vanadium. The peak present at the top-left of Fig.8e is noticeable. It is likely due to porphyrin structures, widely present in the asphaltene fraction. Such contours obtained by SECxRPLC-ICP-MS/MS could be very useful in the future to compare the fractionation performance of SARA process which may vary from one laboratory to another.

4. Conclusion

The objective of this work was to develop a two-dimensional separation method, coupled to elemental detection, for analyzing complex petroleum samples. A high separation power being mandatory for such complex samples, we first evaluated the potential of one-dimensional separation (SEC or RPLC), and then we pointed out that 2D-separations allowed to achieve much higher peak capacities but at the cost of higher dilution. An effective peak capacity of 2600 could indeed be achieved in less than 2.5 h. Both off-line and on-line LCxLC separations were compared using a pareto-optimality approach with the aim of maximizing the peak capacity while minimizing the dilution factor in a given analysis time. The best 2D-conditions in term of peak capacity were found in off-line SEC x RPLC, also considering the huge number of runs required in on-line RPLC x SEC.

To the best of our knowledge, such combination of SEC and RPLC, operated in a comprehensive off-line mode and hyphenated to ICP-MS/MS, is the most advanced tool, without any equivalent in the literature, for the speciation of vanadium, nickel and sulfur in petroleum samples.

SEC as first dimension allows the separation according to the molecular weight of the analytes within a range of 1000 to 30000 g/mol. RPLC as second dimension allows the separation of the molecules according to their hydrophobicity making this coupling very attractive. By coupling these two different retention mechanisms, the species contained in petroleum fractions could be distributed over the entire elution space. This 2D-method hyphenated to ICP-MS/MS could achieve the speciation of vanadium, sulfur and nickel within a single run.

The best 2D-conditions were applied to the characterization of SARA fractions. The metal distribution shows that larger compounds (short retention times in SEC) are more hydrophobic (high retention times in RPLC). Whereas heavy masses are not well separated in SEC alone, they are partly separated in RPLC making the combination of both techniques of great interest.

In the future, it could be possible to apply this analysis method to more complex samples, such as non-fractionated petroleum samples coming from refining units.

References

[1] R. Martínez-Palou, M. de L. Mosqueira, B. Zapata-Rendón, E. Mar-Juárez, C. Bernal-Huicochea, J. de la Cruz Clavel-López, J. Aburto, Transportation of heavy and extra-heavy crude oil by pipeline: A review, J. Pet. Sci. Eng. 75 (2011) 274–282. doi:10.1016/j.petrol.2010.11.020.

[2] S. Gutiérrez Sama, C. Barrère-Mangote, B. Bouyssière, P. Giusti, R. Lobinski, Recent trends in element speciation analysis of crude oils and heavy petroleum fractions, TrAC Trends Anal. Chem. (2017). doi:10.1016/j.trac.2017.10.014.

[3] G. Caumette, C.-P. Lienemann, I. Merdrignac, B. Bouyssiere, R. Lobinski, Element speciation analysis of petroleum and related materials, J. Anal. At. Spectrom. 24 (2009) 263–276. doi:10.1039/B817888G.

[4] M.R. Yakubov, D.V. Milordov, S.G. Yakubova, D.N. Borisov, V.T. Ivanov, K.O. Sinyashin, Concentrations of vanadium and nickel and their ratio in heavy oil asphaltenes, Pet. Chem. 56 (2016) 16–20. doi:10.1134/S0965544116010072.

[5] M.F. Ali, S. Abbas, A review of methods for the demetallization of residual fuel oils, Fuel Process. Technol. 87 (2006) 573–584. doi:10.1016/j.fuproc.2006.03.001.

[6] A.M. McKenna, J.M. Purcell, R.P. Rodgers, A.G. Marshall, Identification of Vanadyl Porphyrins in a Heavy Crude Oil and Raw Asphaltene by Atmospheric Pressure Photoionization Fourier Transform Ion Cyclotron Resonance (FT-ICR) Mass Spectrometry, Energy Fuels. 23 (2009) 2122–2128. doi:10.1021/ef800999e.

[7] X. Zhao, C. Xu, Q. Shi, Porphyrins in Heavy Petroleums: A Review, in: Struct. Model. Complex Pet. Mix., Springer, Cham, 2015: pp. 39–70. doi:10.1007/430_2015_189.

[8] F.G. Wandekoken, C.B. Duyck, T.C.O. Fonseca, T.D. Saint'Pierre, Method for the quantification of vanadyl porphyrins in fractions of crude oils by High Performance Liquid Chromatography–Flow Injection–Inductively Coupled Plasma Mass Spectrometry, Spectrochim. Acta Part B At. Spectrosc. 119 (2016) 1–9. doi:10.1016/j.sab.2016.03.001.

[9] J.S. Ramírez-Pradilla, C. Blanco-Tirado, M. Hubert-Roux, P. Giusti, C. Afonso, M.Y. Combariza, Comprehensive Petroporphyrin Identification in Crude Oils Using Highly Selective Electron Transfer Reactions in MALDI-FTICR-MS, Energy Fuels. 33 (2019) 3899–3907. doi:10.1021/acs.energyfuels.8b04325.

[10] S. Gutiérrez Sama, A. Desprez, G. Krier, C.-P. Lienemann, J. Barbier, R. Lobinski, C. Barrère Mangote, P. Giusti, B. Bouyssiere, Study of the Aggregation of Metal Complexes with Asphaltenes Using Gel Permeation Chromatography Inductively Coupled Plasma High-Resolution Mass Spectrometry, Energy Fuels. 30 (2016). doi:10.1021/acs.energyfuels.6b00559.

[11] A.G. Marshall, R.P. Rodgers, Petroleomics: Chemistry of the underworld, Proc. Natl. Acad. Sci. 105 (2008) 18090–18095. doi:10.1073/pnas.0805069105.

[12] T.A. Maryutina, A.R. Timerbaev, Metal speciation analysis of petroleum: Myth or reality?, Anal. Chim. Acta. 991 (2017) 1–8. doi:10.1016/j.aca.2017.08.036.

[13] G. Gascon, V. Vargas, L. Feo, O. Luisa Castellano, J. Castillo, P. Giusti, S. Acevedo, C.-P. Lienemann, B. Bouyssiere, Size Distributions of Sulfur, Vanadium and Nickel Compounds in Crude Oils, Residues and Their SARA Fractions Determined by Gel Permeation Chromatography Inductively Coupled Plasma High-Resolution Mass Spectrometry, Energy Fuels. 31 (2017). doi:10.1021/acs.energyfuels.7b00527.

[14] S. Acevedo, K. Guzmán, H. Labrador, H. Carrier, B. Bouyssiere, R. Lobinski, Trapping of Metallic Porphyrins by Asphaltene Aggregates: A Size Exclusion Microchromatography

With High-Resolution Inductively Coupled Plasma Mass Spectrometric Detection Study, (2012). doi:10.1021/ef3002857.

[15] P. Pohl, J. Dural, N. Vorapalawut, I. Merdrignac, C.-P. Lienemann, H. Carrier, B. Grassl, B. Bouyssiere, R. Lobinski, Multielement molecular size fractionation in crude oil and oil residue by size exclusion microchromatography with high resolution inductively coupled plasma mass spectrometric detection (HR ICP MS), J. Anal. At. Spectrom. 25 (2010). doi:10.1039/C0JA00076K.

[16] A. Desprez, B. Bouyssiere, C. Arnaudguilhem, G. Krier, L. Vernex-Loset, P. Giusti, Study of the Size Distribution of Sulfur, Vanadium, and Nickel Compounds in Four Crude Oils and Their Distillation Cuts by Gel Permeation Chromatography Inductively Coupled Plasma High-Resolution Mass Spectrometry, Energy Fuels. 28 (2014) 3730–3737. doi:10.1021/ef500571f.

[17] J.-I. Park, A. Al-Mutairi, A.M.J. Marafie, S.-H. Yoon, I. Mochida, X. Ma, The characterization of metal complexes in typical Kuwait atmospheric residues using both GPC coupled with ICP–MS and HT GC–AED, J. Ind. Eng. Chem. 34 (2016) 204–212. doi:10.1016/j.jiec.2015.11.011.

[18] J.C. Putman, S. Gutiérrez Sama, C. Barrère-Mangote, R.P. Rodgers, R. Lobinski, A.G. Marshall, B. Bouyssière, P. Giusti, Analysis of Petroleum Products by Gel Permeation Chromatography Coupled Online with Inductively Coupled Plasma Mass Spectrometry and Offline with Fourier Transform Ion Cyclotron Resonance Mass Spectrometry, Energy Fuels. 32 (2018) 12198–12204. doi:10.1021/acs.energyfuels.8b02788.

[19] A. Vetere, M.W. Alachraf, S.K. Panda, J.T. Andersson, W. Schrader, Studying the fragmentation mechanism of selected components present in crude oil by collision-induced dissociation mass spectrometry, Rapid Commun. Mass Spectrom. 32 (2018) 2141–2151. doi:10.1002/rcm.8280.

[20] E. Magi, C. Ianni, P. Rivaro, R. Frache, Determination of porphyrins and metalloporphyrins using liquid chromatography–diode array detection and mass spectrometry, J. Chromatogr. A. 905 (2001) 141–149. doi:10.1016/S0021-9673(00)01007-4.

[21] T. Loegel, N. Danielson, D. J. Borton, M. Hurt, H. Kenttämaa, Separation of Asphaltenes by Reversed-Phase Liquid Chromatography with Fraction Characterization, Energy Fuels. 26 (2012) 2850–2857. doi:10.1021/ef201919x.

[22] G. Caumette, C.-P. Lienemann, I. Merdrignac, B. Bouyssiere, R. Lobinski, Fractionation and speciation of nickel and vanadium in crude oils by size exclusion chromatography-ICP MS and normal phase HPLC-ICP MS, J. Anal. At. Spectrom. 25 (2010) 1123–1129. doi:10.1039/C003455J.

[23] C.A. Islas-Flores, E. Buenrostro-Gonzalez, C. Lira-Galeana, Fractionation of petroleum resins by normal and reverse phase liquid chromatography, Fuel. 85 (2006) 1842–1850. doi:10.1016/j.fuel.2006.02.007.

[24] B. Klencsár, L. Balcaen, F. Cuyckens, F. Lynen, F. Vanhaecke, Development and validation of a novel quantification approach for gradient elution reversed phase high-performance liquid chromatography coupled to tandem ICP-mass spectrometry (RP-HPLC-ICP-MS/MS) and its application to diclofenac and its related compounds, Anal. Chim. Acta. 974 (2017) 43–53. doi:10.1016/j.aca.2017.04.030.

[25] B. Meermann, M. Kießhauer, Development of an oxygen-gradient system to overcome plasma instabilities during HPLC/ICP-MS measurements using gradient elution, J. Anal. At. Spectrom. 26 (2011) 2069–2075. doi:10.1039/C1JA10177C.

608 [26] L. Rottmann, K.G. Heumann, Development of an on-line isotope dilution technique
609 with HPLC/ICP-MS for the accurate determination of elemental species, Fresenius J.
610 Anal. Chem. 350 (1994) 221–227. doi:10.1007/BF00322473.
611 [27] B. Klencsár, S. Li, L. Balcaen, F. Vanhaecke, High-performance liquid chromatography
612 coupled to inductively coupled plasma – Mass spectrometry (HPLC-ICP-MS) for
613 quantitative metabolite profiling of non-metal drugs, TrAC Trends Anal. Chem. 104
614 (2018) 118–134. doi:10.1016/j.trac.2017.09.020.
615 [28] C. Siethoff, I. Feldmann, N. Jakubowski, M. Linscheid, Quantitative determination of
616 DNA adducts using liquid chromatography/electrospray ionization mass spectrometry
617 and liquid chromatography/high-resolution inductively coupled plasma mass
618 spectrometry, J. Mass Spectrom. 34 (1999) 421–426. doi:10.1002/(SICI)1096-
619 9888(199904)34:4<421::AID-JMS790>3.0.CO;2-I.
620 [29] A.S. Pereira, M. Schelfaut, F. Lynen, P. Sandra, Design and evaluation of a multi-
621 detection system composed of ultraviolet, evaporative light scattering and inductively
622 coupled plasma mass spectrometry detection for the analysis of pharmaceuticals by
623 liquid chromatography, J. Chromatogr. A. 1185 (2008) 78–84.
624 doi:10.1016/j.chroma.2008.01.030.
625 [30] G. Koellensperger, S. Hann, J. Nurmi, T. Prohaska, G. Stingeder, Uncertainty of species
626 unspecific quantification strategies in hyphenated ICP-MS analysis, J. Anal. At. Spectrom.
627 18 (2003) 1047–1055. doi:10.1039/B302565A.
628 [31] M. Sarrut, A. D'Attoma, S. Heinisch, Optimization of conditions in on-line
629 comprehensive two-dimensional reversed phase liquid chromatography. Experimental
630 comparison with one-dimensional reversed phase liquid chromatography for the
631 separation of peptides, J. Chromatogr. A. 1421 (2015) 48–59.
632 doi:10.1016/j.chroma.2015.08.052.
633 [32] M. Sarrut, F. Rouvière, S. Heinisch, Theoretical and experimental comparison of one
634 dimensional versus on-line comprehensive two dimensional liquid chromatography for
635 optimized sub-hour separations of complex peptide samples, J. Chromatogr. A. 1498
636 (2017) 183–195. doi:10.1016/j.chroma.2017.01.054.
637 [33] K.M. Kalili, A. de Villiers, Systematic optimisation and evaluation of on-line, off-line
638 and stop-flow comprehensive hydrophilic interaction chromatography × reversed phase
639 liquid chromatographic analysis of procyanidins, Part I: Theoretical considerations, J.
640 Chromatogr. A. 1289 (2013) 58–68. doi:10.1016/j.chroma.2013.03.008.
641 [34] M. Iguiniz, S. Heinisch, Two-dimensional liquid chromatography in pharmaceutical
642 analysis. Instrumental aspects, trends and applications, J. Pharm. Biomed. Anal. 145
643 (2017) 482–503.
644 [35] M. Bernardin, F. Bessueille-Barbier, A. Le Masle, C.-P. Lienemann, S. Heinisch,
645 Suitable interface for coupling liquid chromatography to inductively coupled plasma-
646 mass spectrometry for the analysis of organic matrices. 1 Theoretical and experimental
647 considerations on solute dispersion, J. Chromatogr. A. 1565 (2018) 68–80.
648 doi:10.1016/j.chroma.2018.06.024.
649 [36] M. Bernardin, F. Bessueille-Barbier, A. Le Masle, C.-P. Lienemann, S. Heinisch,
650 Suitable interface for coupling liquid chromatography to inductively coupled plasma-
651 mass spectrometry for the analysis of organic matrices. 2 Comparison of Sample
652 Introduction Systems, J. Chromatogr. A. (2019). doi:10.1016/j.chroma.2019.04.074.

[37] J.C. Giddings, Maximum number of components resolvable by gel filtration and other elution chromatographic methods, Anal. Chem. 39 (1967) 1027–1028. doi:10.1021/ac60252a025.

[38] U.D. Neue, Theory of peak capacity in gradient elution, J. Chromatogr. A. 1079 (2005) 153–161. doi:10.1016/j.chroma.2005.03.008.

[39] L.R. Snyder, J.W. Dolan, J.R. Gant, Gradient elution in high-performance liquid chromatography : I. Theoretical basis for reversed-phase systems, J. Chromatogr. A. 165 (1979) 3–30. doi:10.1016/S0021-9673(00)85726-X.

[40] L. Hagel, Peak capacity of columns for size-exclusion chromatography, J. Chromatogr. A. 591 (1992) 47–54. doi:10.1016/0021-9673(92)80221-F.

[41] F. Bedani, Theories to support method development in comprehensive two-dimensional liquid chromatography – A review Filippo Bedani1,2,*, Peter J. Schoenmakers1 and Hans-Gerd Janssen1,3, (n.d.).

[42] A. D'Attoma, C. Grivel, S. Heinisch, On-line comprehensive two-dimensional separations of charged compounds using reversed-phase high performance liquid chromatography and hydrophilic interaction chromatography. Part I: Orthogonality and practical peak capacity considerations, J. Chromatogr. A. 1262 (2012) 148–159. doi:10.1016/j.chroma.2012.09.028.

[43] M.A. Stadalius, H.S. Gold, L.R. Snyder, Optimization model for the gradient elution separation of peptide mixtures by reversed-phase high-performance liquid chromatography : Verification of retention relationships, J. Chromatogr. A. 296 (1984) 31–59. doi:10.1016/S0021-9673(01)96400-3.

[44] C. Berrueco, S. Venditti, T.J. Morgan, P. Álvarez, M. Millan, A.A. Herod, R. Kandiyoti, Calibration of Size-Exclusion Chromatography Columns with 1-Methyl-2-pyrrolidinone (NMP)/Chloroform Mixtures as Eluent: Applications to Petroleum-Derived Samples, Energy Fuels. 22 (2008) 3265–3274. doi:10.1021/ef8003703.

[45] E. Reingruber, J.J. Jansen, W. Buchberger, P. Schoenmakers, Transfer-volume effects in two-dimensional chromatography: Adsorption-phenomena in second-dimension size-exclusion chromatography, J. Chromatogr. A. 1218 (2011) 1147–1152. doi:10.1016/j.chroma.2010.12.080.

Figure Captions

Figure 1: Scheme of the SARA fractionation of a vacuum residue (VR).

Figure 2: Schematic representation of the instrument setup in off-line SECxRPLC-ICP-MS/MS (tubing dimensions are given in the experimental section).

Figure 3: Overlaid separations of an atmospheric residue (AR Venezuela) in SEC-ICP-MS/MS with specific detection of sulfur, vanadium and nickel. Conditions: (a) APC XT 45 column (150 x 4.6 mm, 1.7 µm) and (b) APC XT 125 column (150 x 4.6 mm, 2.5 µm). Other conditions given in the experimental section.

Figure 4: Separation of 8 polystyrene standards (contained in 2 different solutions) in SEC-UV (254 nm). The green dotted curve represents the SEC calibration curve. Conditions: APC XT 125 column (150 x 4.6 mm, 2.5 µm). 5 µL injected. Other conditions given in the experimental section.

Figure 5: Overlaid separations of SARA fractions in (a, b, c) SEC-ICP-MS/MS and in (d, e, f) RPLC-ICP-MS/MS with specific detection of (a, d) Sulfur, (b, e) Vanadium and (c, f) Nickel. SEC conditions: APC XT 125 (150 x 4.6 mm, 2.5 µm) column; Mobile phase: THF. 0.8 mL/min; 30 °C; 15 µL injected. RPLC conditions: Acquity BEH C18 (50 x 2.1 mm, 1.7 µm) column; A: 80/20 ACN/H_2O; B: THF; 1 % B to 99 % B in 15.2 min; 0.8 mL/min; 30 °C; 5 µL injected. Flow splitter prior to ICP-MS/MS (1:1). Peak of 2,3,7,8,12,13,17,18-Octaethyl-21H,23H-porphin in grey dotted line.

Figure 6: Full pareto plots (red triangles) of dilution factor versus effective peak capacity for an analysis time of 150 min in on-line RPLCxSEC (γ=1). The pareto-optimal front is represented in red dotted line. The conditions of setting #1 to #5 are listed in Table 1. The

711 blue circle corresponds to the optimized set of conditions in off-line SECxRPLC (listed in Table
712 2). See text for more explanations.

713

714 Figure 7: SECxRPLC-ICP-MS/MS analysis of SARA fractions with specific detection, of (a, b, c)
715 Sulfur and (d, e, f) Vanadium: (a, d) aromatic, (b, e) resin and (c, f) asphaltene fractions. See
716 conditions in Table 2.

717

718 Figure 8: Overlay of the SECxRPLC-contours of aromatic (green, dotted line), resins (blue,
719 solid line) and asphaltene (red, dashed line) fractions with ICP-MS/MS specific detection of
720 (a) Sulfur and (b) Vanadium. See conditions in Table 2.

Figure 1

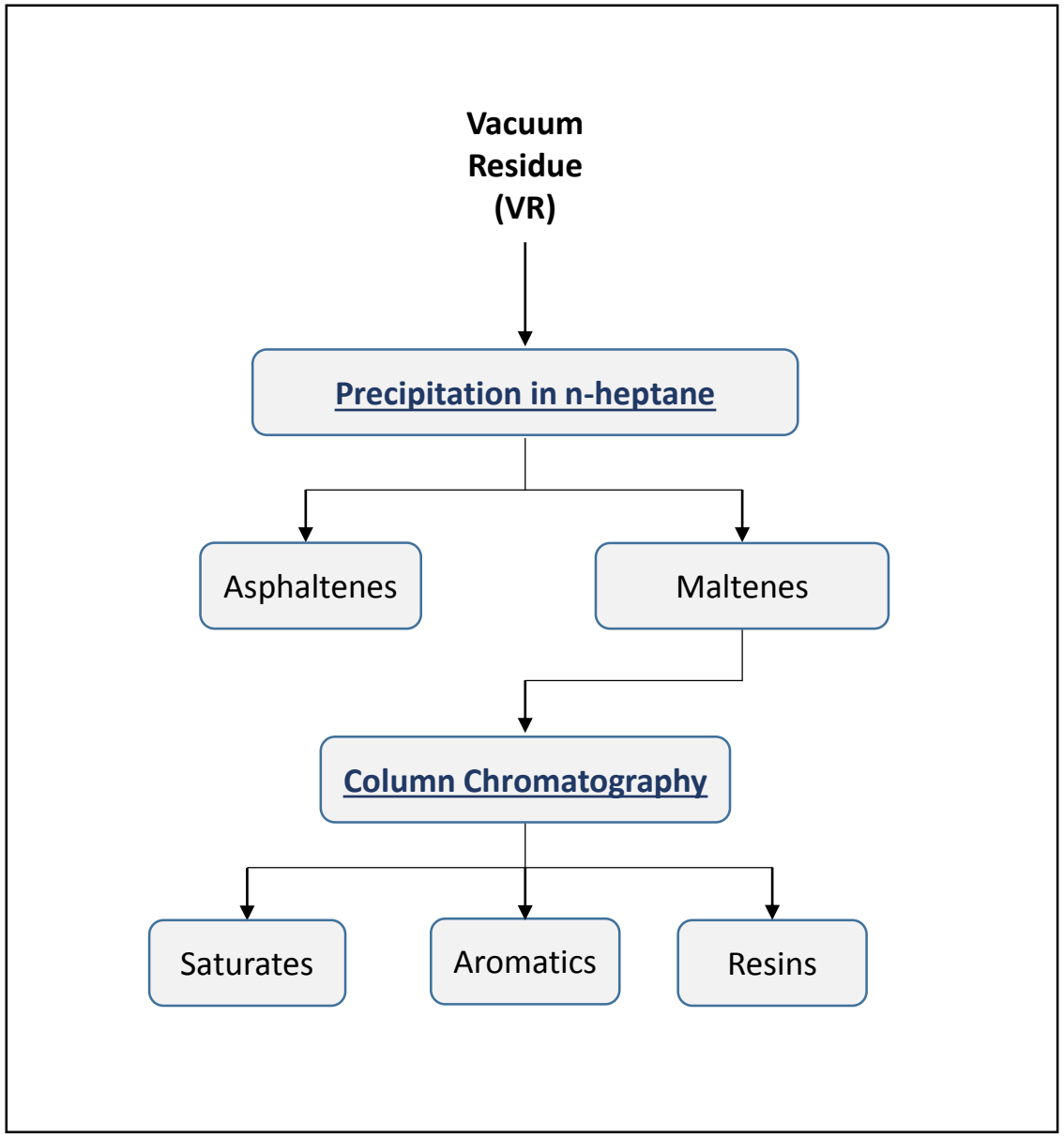
Vacuum Residue (VR)
Precipitation in n-heptane
Asphaltenes
Maltenes
Column Chromatography
Saturates
Aromatics
Resins

Figure 2

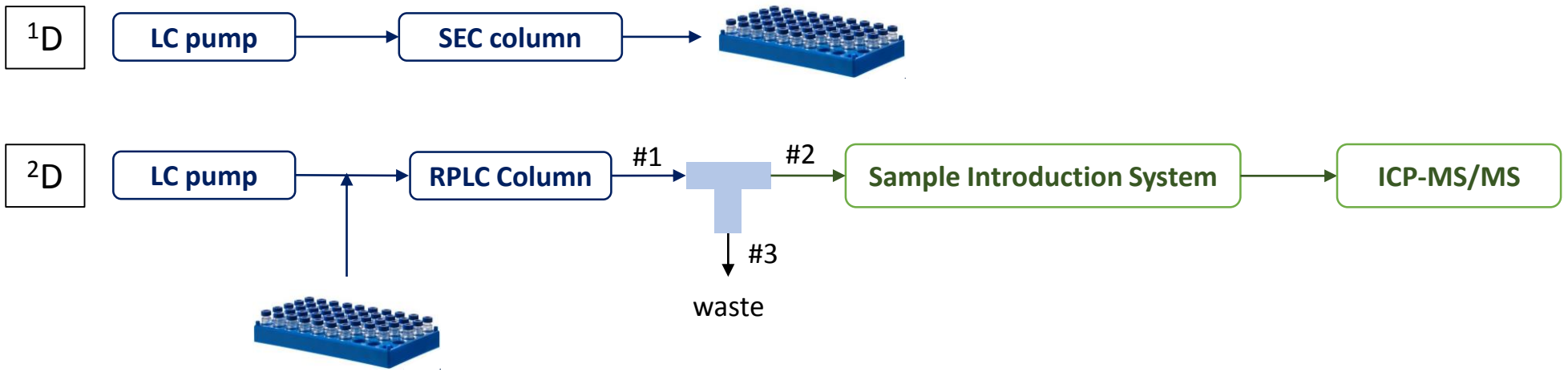
1D
LC pump
SEC column
2D
LC pump
RPLC Column
#1
#2
#3
Sample Introduction System
ICP-MS/MS
waste

Figure 3

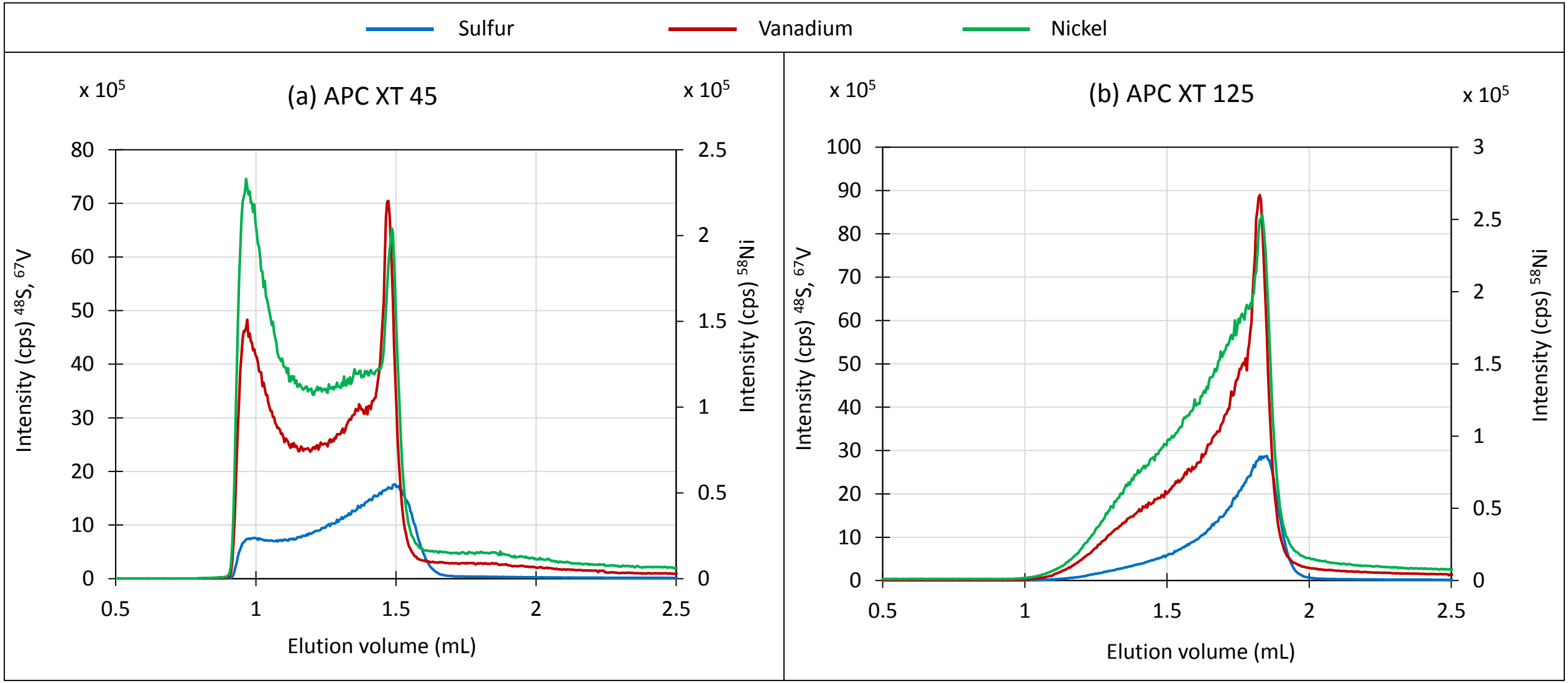
Sulfur
Vanadium
Nickel
(a) APC XT 45
x 10^5
x 10^5
Intensity (cps) 48S, 67V
Intensity (cps) 58Ni
Elution volume (mL)
(b) APC XT 125
x 10^5
x 10^5
Intensity (cps) 48S, 67V
Intensity (cps) 58Ni
Elution volume (mL)

Figure 4

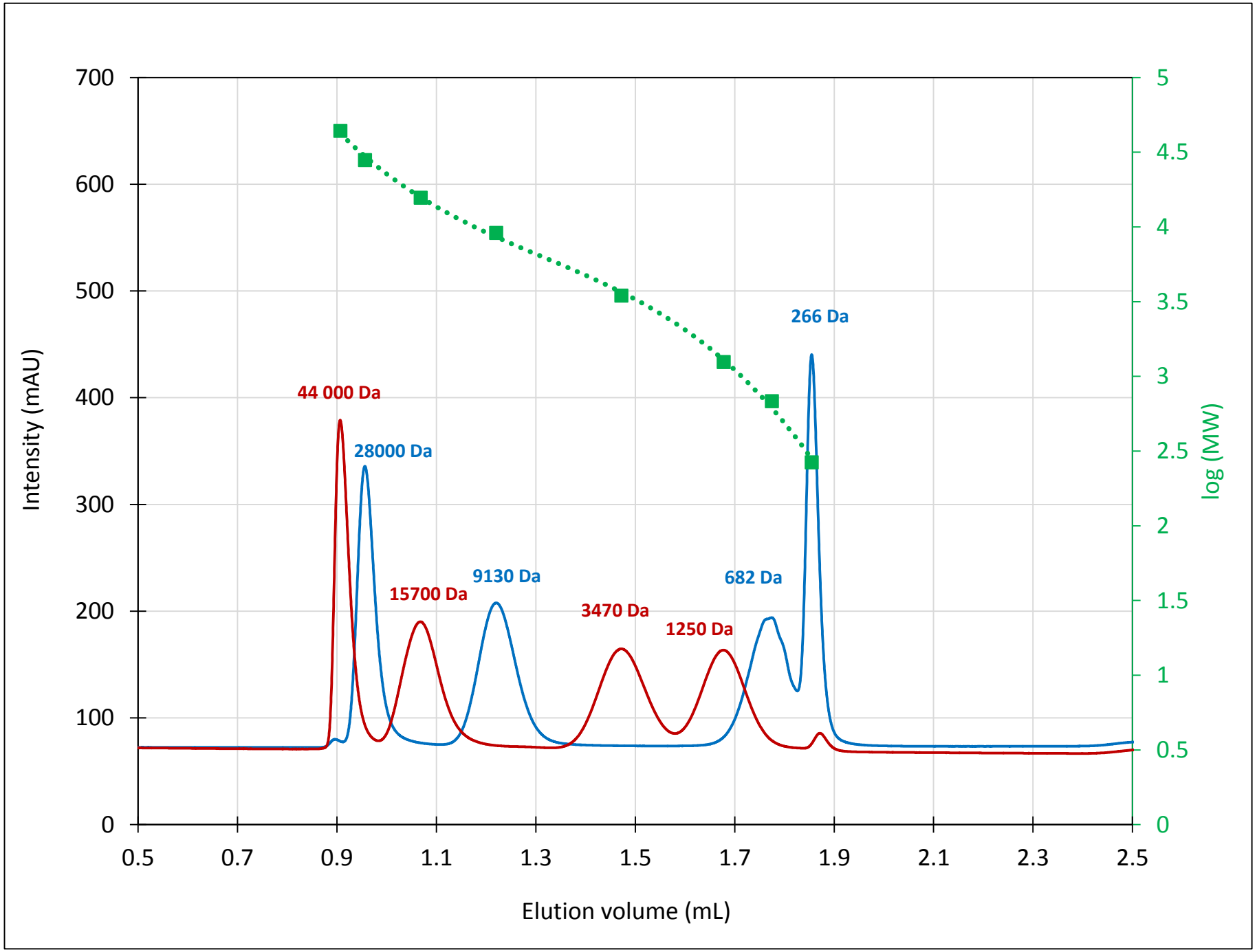
700
600
500
400
300
200
100
0
Intensity (mAU)
5
4.5
4
3.5
3
2.5
2
1.5
1
0.5
0
log (MW)
0.5
0.7
0.9
1.1
1.3
1.5
1.7
1.9
2.1
2.3
2.5
Elution volume (mL)
44 000 Da
28000 Da
15700 Da
9130 Da
3470 Da
1250 Da
682 Da
266 Da

Figure 5

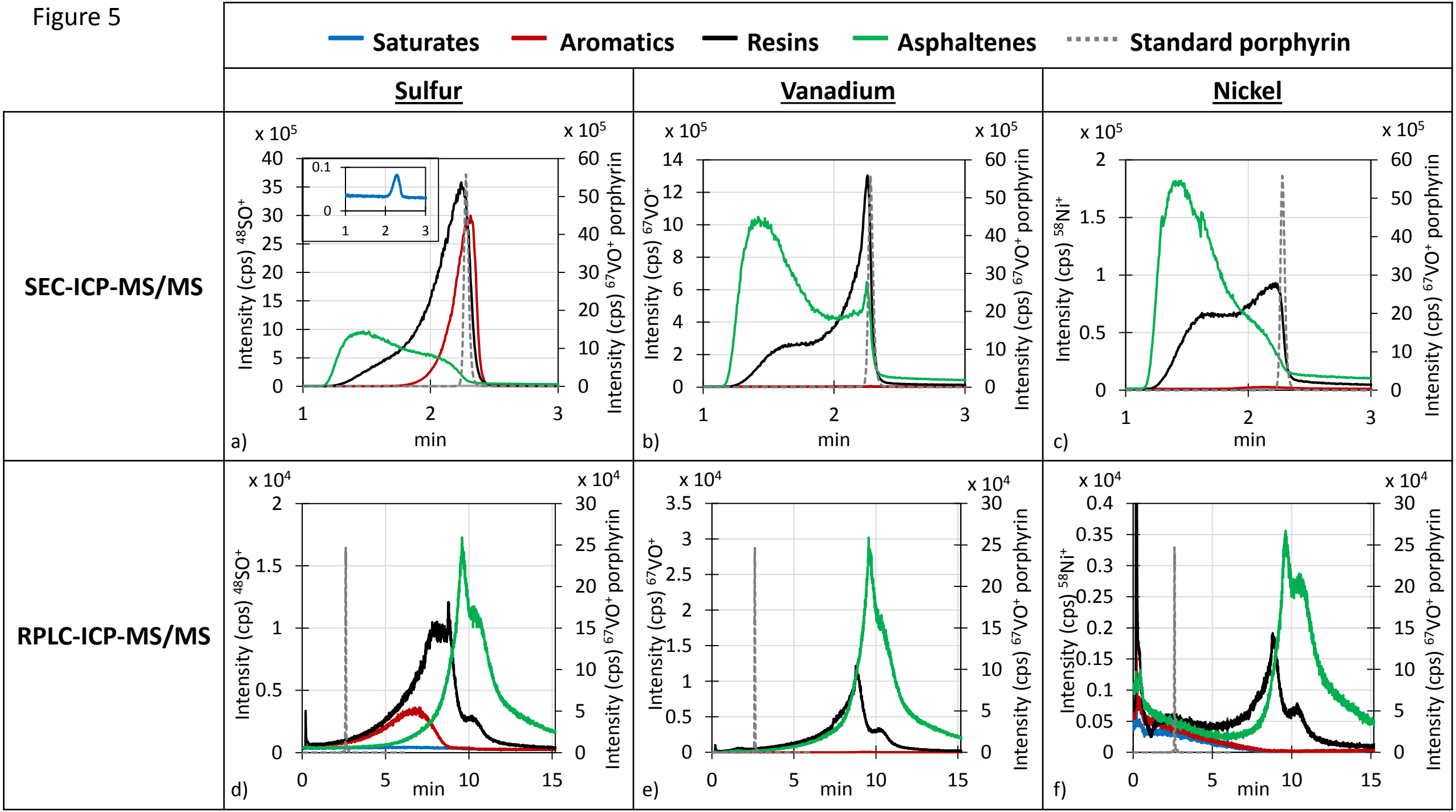
Saturates
Aromatics
Resins
Asphaltenes
Standard porphyrin
Sulfur
Vanadium
Nickel
SEC-ICP-MS/MS
RPLC-ICP-MS/MS
Intensity (cps) 48SO+
Intensity (cps) 67VO+
Intensity (cps) 58Ni+
Intensity (cps) 67VO+ porphyrin
min
a)
b)
c)
d)
e)
f)

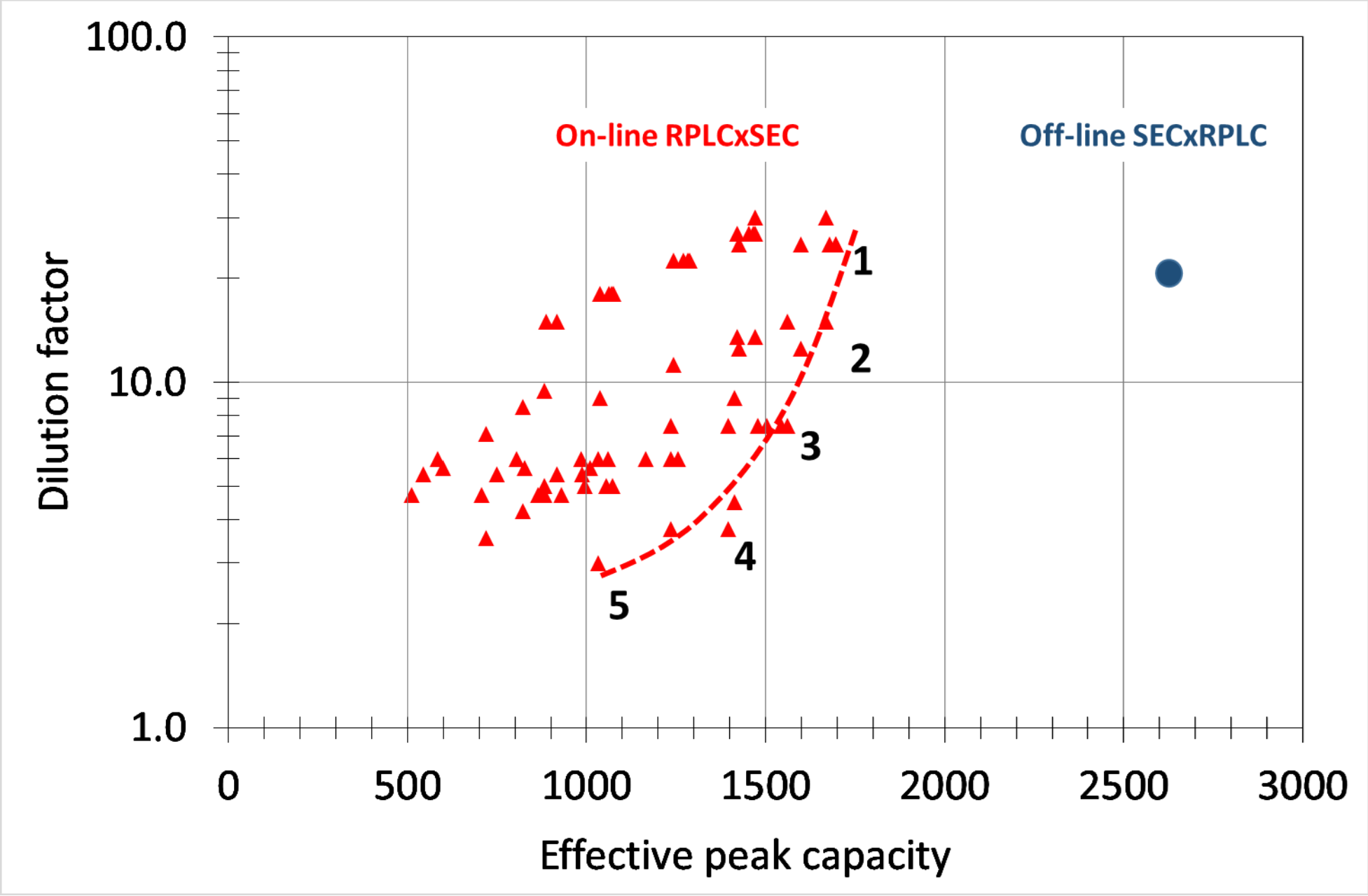
100.0
10.0
1.0
Dilution factor
On-line RPLCxSEC
Off-line SECxRPLC
1
2
3
4
5
0
500
1000
1500
2000
2500
3000
Effective peak capacity

Figure 6

Figure 7

	Sulfur	**Vanadium**
Aromatics	(a) 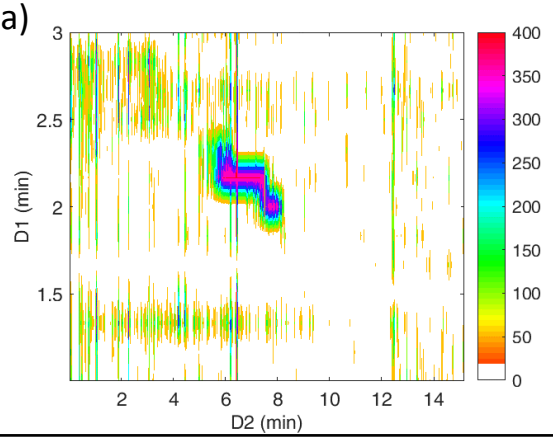	(d) *Not detected*
Resins	(b) 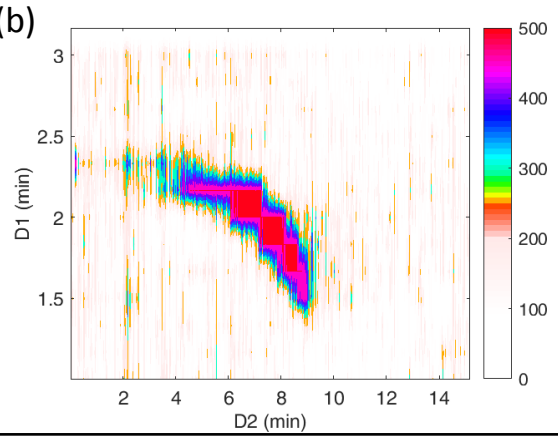	(e) 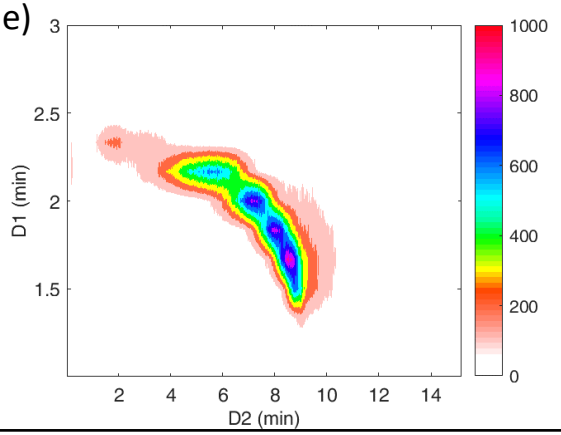
Asphaltenes	(c) 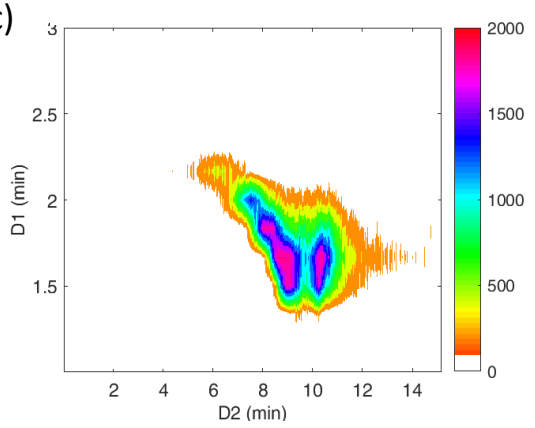	(f) 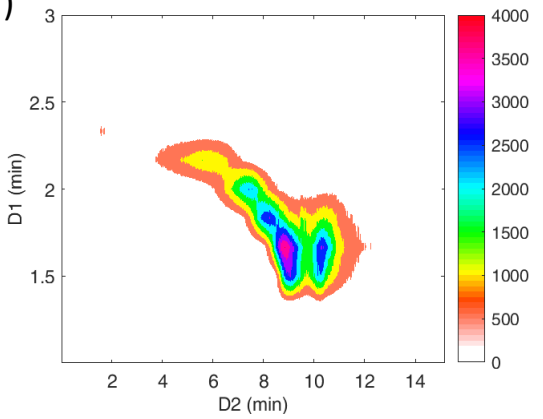

Figure 8

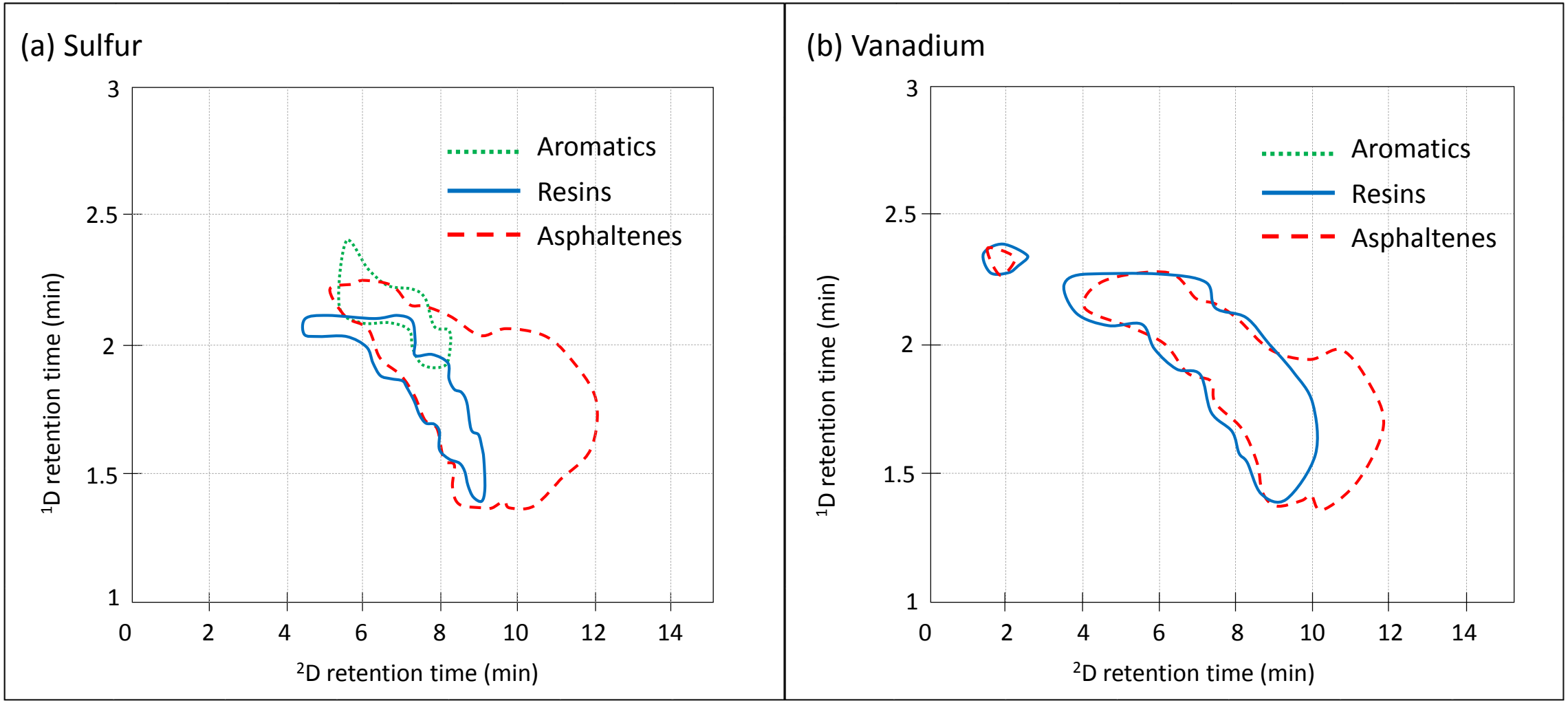
(a) Sulfur
Aromatics
Resins
Asphaltenes
3
2.5
2
1.5
1
0
2
4
6
8
10
12
14
1D retention time (min)
2D retention time (min)
(b) Vanadium
Aromatics
Resins
Asphaltenes
3
2.5
2
1.5
1
0
2
4
6
8
10
12
14
1D retention time (min)
2D retention time (min)